Supporting Information

Data-Efficient Training of Machine Learning Interatomic Potentials for MAX-Phase Synthesizability Prediction

Jonghyuk Kim[1,2], Woojin Shin[2], Jungjae Hwang[2], Junghyeon Kwon[1,2], Sanghyeon Song[2] and Kyoungmin Min[2,*]

[1]School of Mechanical Engineering, Soongsil University, 369 Sangdo-ro, Dongjak-gu, Seoul 06978, Republic of Korea

[2]School of Mechanical Engineering, Yonsei University, 50 Yonsei-ro, Seodaemun-gu, Seoul 03722, Republic of Korea

*Corresponding author: Kyoungmin Min (kmin.min@yonsei.ac.kr)

ESI 1. The high-entropy MAX phase candidates consist of four types: 4_M_2AC, 4_M_3AC_2, 5_M_2AC, and 5_M_3AC_2. Each category includes 140, 140, 112, and 112 chemical formulas, respectively, resulting in a total of 504 compositions. Formation energy (eV/atom) values are also provided for all compositions, and all candidates exhibit formation energies lower than −0.6116 eV/atom, indicating structural stability. These compositions were constructed as follows.

Table S1. 4_M_2AC HE-MAX candidates (Index 1–140; N = 140) with compositions and formation energies (Ef, eV/atom) used for thermodynamic stability screening.

Index Number	Formula	Formation Energy (eV/atom)	Index Number	Formula	Formation Energy (eV/atom)
1	Ti0.5V0.5Cr0.5Zr0.5AlC	-0.9251	71	V0.5Cr0.5Zr0.5Nb0.5AlC	-0.8607
2	Ti0.5V0.5Cr0.5Zr0.5SiC	-0.9654	72	V0.5Cr0.5Zr0.5Nb0.5SiC	-0.8828
3	Ti0.5V0.5Cr0.5Nb0.5AlC	-0.9134	73	V0.5Cr0.5Zr0.5Mo0.5AlC	-1.2447
4	Ti0.5V0.5Cr0.5Nb0.5SiC	-0.9411	74	V0.5Cr0.5Zr0.5Mo0.5SiC	-1.2402
5	Ti0.5V0.5Cr0.5Mo0.5AlC	-1.3075	75	V0.5Cr0.5Zr0.5Hf0.5AlC	-0.9011
6	Ti0.5V0.5Cr0.5Mo0.5SiC	-1.3061	76	V0.5Cr0.5Zr0.5Hf0.5SiC	-0.9295
7	Ti0.5V0.5Cr0.5Hf0.5AlC	-0.9463	77	V0.5Cr0.5Zr0.5Ta0.5AlC	-0.8683
8	Ti0.5V0.5Cr0.5Hf0.5SiC	-0.9599	78	V0.5Cr0.5Zr0.5Ta0.5SiC	-0.8816
9	Ti0.5V0.5Cr0.5Ta0.5AlC	-0.9255	79	V0.5Cr0.5Nb0.5Mo0.5AlC	-1.2177
10	Ti0.5V0.5Cr0.5Ta0.5SiC	-0.9276	80	V0.5Cr0.5Nb0.5Mo0.5SiC	-1.2017
11	Ti0.5V0.5Zr0.5Nb0.5AlC	-0.7847	81	V0.5Cr0.5Nb0.5Hf0.5AlC	-0.8822
12	Ti0.5V0.5Zr0.5Nb0.5SiC	-0.8322	82	V0.5Cr0.5Nb0.5Hf0.5SiC	-0.8835
13	Ti0.5V0.5Zr0.5Mo0.5AlC	-1.1629	83	V0.5Cr0.5Nb0.5Ta0.5AlC	-0.8464
14	Ti0.5V0.5Zr0.5Mo0.5SiC	-1.1896	84	V0.5Cr0.5Nb0.5Ta0.5SiC	-0.8181
15	Ti0.5V0.5Zr0.5Hf0.5AlC	-0.7991	85	V0.5Cr0.5Mo0.5Hf0.5AlC	-1.2697
16	Ti0.5V0.5Zr0.5Hf0.5SiC	-0.8857	86	V0.5Cr0.5Mo0.5Hf0.5SiC	-1.2522
17	Ti0.5V0.5Zr0.5Ta0.5AlC	-0.7927	87	V0.5Cr0.5Mo0.5Ta0.5AlC	-1.2275
18	Ti0.5V0.5Zr0.5Ta0.5SiC	-0.8486	88	V0.5Cr0.5Mo0.5Ta0.5SiC	-1.2126
19	Ti0.5V0.5Nb0.5Mo0.5AlC	-1.1460	89	V0.5Cr0.5Hf0.5Ta0.5AlC	-0.8823
20	Ti0.5V0.5Nb0.5Mo0.5SiC	-1.1489	90	V0.5Cr0.5Hf0.5Ta0.5SiC	-0.9139

21	Ti0.5V0.5Nb0.5Hf0.5AlC	-0.7956	91	V0.5Zr0.5Nb0.5Mo0.5AlC	-1.1010
22	Ti0.5V0.5Nb0.5Hf0.5SiC	-0.8570	92	V0.5Zr0.5Nb0.5Mo0.5SiC	-1.1119
23	Ti0.5V0.5Nb0.5Ta0.5AlC	-0.7732	93	V0.5Zr0.5Nb0.5Hf0.5AlC	-0.7636
24	Ti0.5V0.5Nb0.5Ta0.5SiC	-0.7928	94	V0.5Zr0.5Nb0.5Hf0.5SiC	-0.8373
25	Ti0.5V0.5Mo0.5Hf0.5AlC	-1.1793	95	V0.5Zr0.5Nb0.5Ta0.5AlC	-0.7348
26	Ti0.5V0.5Mo0.5Hf0.5SiC	-1.2140	96	V0.5Zr0.5Nb0.5Ta0.5SiC	-0.7702
27	Ti0.5V0.5Mo0.5Ta0.5AlC	-1.1549	97	V0.5Zr0.5Mo0.5Hf0.5AlC	-1.1453
28	Ti0.5V0.5Mo0.5Ta0.5SiC	-1.1593	98	V0.5Zr0.5Mo0.5Hf0.5SiC	-1.1959
29	Ti0.5V0.5Hf0.5Ta0.5AlC	-0.8114	99	V0.5Zr0.5Mo0.5Ta0.5AlC	-1.1063
30	Ti0.5V0.5Hf0.5Ta0.5SiC	-0.8692	100	V0.5Zr0.5Mo0.5Ta0.5SiC	-1.1235
31	Ti0.5Cr0.5Zr0.5Nb0.5AlC	-0.7298	101	V0.5Zr0.5Hf0.5Ta0.5AlC	-0.7806
32	Ti0.5Cr0.5Zr0.5Nb0.5SiC	-0.7444	102	V0.5Zr0.5Hf0.5Ta0.5SiC	-0.8399
33	Ti0.5Cr0.5Zr0.5Mo0.5AlC	-1.1037	103	V0.5Nb0.5Mo0.5Hf0.5AlC	-1.1180
34	Ti0.5Cr0.5Zr0.5Mo0.5SiC	-1.1107	104	V0.5Nb0.5Mo0.5Hf0.5SiC	-1.1412
35	Ti0.5Cr0.5Zr0.5Hf0.5AlC	-0.7528	105	V0.5Nb0.5Mo0.5Ta0.5AlC	-1.0736
36	Ti0.5Cr0.5Zr0.5Hf0.5SiC	-0.8120	106	V0.5Nb0.5Mo0.5Ta0.5SiC	-1.0623
37	Ti0.5Cr0.5Zr0.5Ta0.5AlC	-0.7244	107	V0.5Nb0.5Hf0.5Ta0.5AlC	-0.7515
38	Ti0.5Cr0.5Zr0.5Ta0.5SiC	-0.7609	108	V0.5Nb0.5Hf0.5Ta0.5SiC	-0.7923
39	Ti0.5Cr0.5Nb0.5Mo0.5AlC	-1.0790	109	V0.5Mo0.5Hf0.5Ta0.5AlC	-1.1256
40	Ti0.5Cr0.5Nb0.5Mo0.5SiC	-1.0762	110	V0.5Mo0.5Hf0.5Ta0.5SiC	-1.1377
41	Ti0.5Cr0.5Nb0.5Hf0.5AlC	-0.7358	111	Cr0.5Zr0.5Nb0.5Mo0.5AlC	-1.0309
42	Ti0.5Cr0.5Nb0.5Hf0.5SiC	-0.7640	112	Cr0.5Zr0.5Nb0.5Mo0.5SiC	-1.0400
43	Ti0.5Cr0.5Nb0.5Ta0.5AlC	-0.7126	113	Cr0.5Zr0.5Nb0.5Hf0.5AlC	-0.7039
44	Ti0.5Cr0.5Nb0.5Ta0.5SiC	-0.7255	114	Cr0.5Zr0.5Nb0.5Hf0.5SiC	-0.7581
45	Ti0.5Cr0.5Mo0.5Hf0.5AlC	-1.1162	115	Cr0.5Zr0.5Nb0.5Ta0.5AlC	-0.6771
46	Ti0.5Cr0.5Mo0.5Hf0.5SiC	-1.1158	116	Cr0.5Zr0.5Nb0.5Ta0.5SiC	-0.6920
47	Ti0.5Cr0.5Mo0.5Ta0.5AlC	-1.0946	117	Cr0.5Zr0.5Mo0.5Hf0.5AlC	-1.0798
48	Ti0.5Cr0.5Mo0.5Ta0.5SiC	-1.0745	118	Cr0.5Zr0.5Mo0.5Hf0.5SiC	-1.1192
49	Ti0.5Cr0.5Hf0.5Ta0.5AlC	-0.7515	119	Cr0.5Zr0.5Mo0.5Ta0.5AlC	-1.0407
50	Ti0.5Cr0.5Hf0.5Ta0.5SiC	-0.7803	120	Cr0.5Zr0.5Mo0.5Ta0.5SiC	-1.0437
51	Ti0.5Zr0.5Nb0.5Mo0.5AlC	-0.9680	121	Cr0.5Zr0.5Hf0.5Ta0.5AlC	-0.7098

52	Ti0.5Zr0.5Nb0.5Mo0.5SiC	-1.0094	122	Cr0.5Zr0.5Hf0.5Ta0.5SiC	-0.7589
53	Ti0.5Zr0.5Nb0.5Hf0.5AlC	-0.6274	123	Cr0.5Nb0.5Mo0.5Hf0.5AlC	-1.0451
54	Ti0.5Zr0.5Nb0.5Hf0.5SiC	-0.7244	124	Cr0.5Nb0.5Mo0.5Hf0.5SiC	-1.0380
55	Ti0.5Zr0.5Nb0.5Ta0.5AlC	-0.6116	125	Cr0.5Nb0.5Mo0.5Ta0.5AlC	-1.0065
56	Ti0.5Zr0.5Nb0.5Ta0.5SiC	-0.6635	126	Cr0.5Nb0.5Mo0.5Ta0.5SiC	-1.0053
57	Ti0.5Zr0.5Mo0.5Hf0.5AlC	-1.0142	127	Cr0.5Nb0.5Hf0.5Ta0.5AlC	-0.6839
58	Ti0.5Zr0.5Mo0.5Hf0.5SiC	-1.0666	128	Cr0.5Nb0.5Hf0.5Ta0.5SiC	-0.6964
59	Ti0.5Zr0.5Mo0.5Ta0.5AlC	-0.9784	129	Cr0.5Mo0.5Hf0.5Ta0.5AlC	-1.0567
60	Ti0.5Zr0.5Mo0.5Ta0.5SiC	-1.0127	130	Cr0.5Mo0.5Hf0.5Ta0.5SiC	-1.0657
61	Ti0.5Zr0.5Hf0.5Ta0.5AlC	-0.6390	131	Zr0.5Nb0.5Mo0.5Hf0.5AlC	-0.9639
62	Ti0.5Zr0.5Hf0.5Ta0.5SiC	-0.7335	132	Zr0.5Nb0.5Mo0.5Hf0.5SiC	-1.0098
63	Ti0.5Nb0.5Mo0.5Hf0.5AlC	-0.9870	133	Zr0.5Nb0.5Mo0.5Ta0.5AlC	-0.9191
64	Ti0.5Nb0.5Mo0.5Hf0.5SiC	-1.0223	134	Zr0.5Nb0.5Mo0.5Ta0.5SiC	-0.9303
65	Ti0.5Nb0.5Mo0.5Ta0.5AlC	-0.9498	135	Zr0.5Nb0.5Hf0.5Ta0.5AlC	-0.6125
66	Ti0.5Nb0.5Mo0.5Ta0.5SiC	-0.9518	136	Zr0.5Nb0.5Hf0.5Ta0.5SiC	-0.6628
67	Ti0.5Nb0.5Hf0.5Ta0.5AlC	-0.6306	137	Zr0.5Mo0.5Hf0.5Ta0.5AlC	-0.9723
68	Ti0.5Nb0.5Hf0.5Ta0.5SiC	-0.6741	138	Zr0.5Mo0.5Hf0.5Ta0.5SiC	-1.0177
69	Ti0.5Mo0.5Hf0.5Ta0.5AlC	-1.0007	139	Nb0.5Mo0.5Hf0.5Ta0.5AlC	-0.9320
70	Ti0.5Mo0.5Hf0.5Ta0.5SiC	-1.0227	140	Nb0.5Mo0.5Hf0.5Ta0.5SiC	-0.9440

Table S2. 4_M_3AC_2 HE-MAX candidates (Index 141–280; N = 140) with compositions and formation energies (Ef, eV/atom) used for thermodynamic stability screening.

Index Number	Formula	Formation Energy (eV/atom)	Index Number	Formula	Formation Energy (eV/atom)
141	Ti0.75V0.75Cr0.75Zr0.75AlC2	-0.9149	211	V0.75Cr0.75Zr0.75Nb0.75AlC2	-0.8471
142	Ti0.75V0.75Cr0.75Zr0.75SiC2	-0.9333	212	V0.75Cr0.75Zr0.75Nb0.75SiC2	-0.8376
143	Ti0.75V0.75Cr0.75Nb0.75AlC2	-0.9061	213	V0.75Cr0.75Zr0.75Mo0.75AlC2	-1.2029
144	Ti0.75V0.75Cr0.75Nb0.75SiC2	-0.9047	214	V0.75Cr0.75Zr0.75Mo0.75SiC2	-1.1737
145	Ti0.75V0.75Cr0.75Mo0.75AlC2	-1.2794	215	V0.75Cr0.75Zr0.75Hf0.75AlC2	-0.8992
146	Ti0.75V0.75Cr0.75Mo0.75SiC2	-1.2668	216	V0.75Cr0.75Zr0.75Hf0.75SiC2	-0.9312
147	Ti0.75V0.75Cr0.75Hf0.75AlC2	-0.9464	217	V0.75Cr0.75Zr0.75Ta0.75AlC2	-0.8747
148	Ti0.75V0.75Cr0.75Hf0.75SiC2	-0.9473	218	V0.75Cr0.75Zr0.75Ta0.75SiC2	-0.8561
149	Ti0.75V0.75Cr0.75Ta0.75AlC2	-0.9310	219	V0.75Cr0.75Nb0.75Mo0.75AlC2	-1.1606
150	Ti0.75V0.75Cr0.75Ta0.75SiC2	-0.9343	220	V0.75Cr0.75Nb0.75Mo0.75SiC2	-1.1480
151	Ti0.75V0.75Zr0.75Nb0.75AlC2	-0.7963	221	V0.75Cr0.75Nb0.75Hf0.75AlC2	-0.8607
152	Ti0.75V0.75Zr0.75Nb0.75SiC2	-0.8266	222	V0.75Cr0.75Nb0.75Hf0.75SiC2	-0.8448
153	Ti0.75V0.75Zr0.75Mo0.75AlC2	-1.1666	223	V0.75Cr0.75Nb0.75Ta0.75AlC2	-0.8268
154	Ti0.75V0.75Zr0.75Mo0.75SiC2	-1.1719	224	V0.75Cr0.75Nb0.75Ta0.75SiC2	-0.7978
155	Ti0.75V0.75Zr0.75Hf0.75AlC2	-0.8558	225	V0.75Cr0.75Mo0.75Hf0.75AlC2	-1.2052
156	Ti0.75V0.75Zr0.75Hf0.75SiC2	-0.9060	226	V0.75Cr0.75Mo0.75Hf0.75SiC2	-1.1954
157	Ti0.75V0.75Zr0.75Ta0.75AlC2	-0.8163	227	V0.75Cr0.75Mo0.75Ta0.75AlC2	-1.1828
158	Ti0.75V0.75Zr0.75Ta0.75SiC2	-0.8529	228	V0.75Cr0.75Mo0.75Ta0.75SiC2	-1.1546
159	Ti0.75V0.75Nb0.75Mo0.75AlC2	-1.1378	229	V0.75Cr0.75Hf0.75Ta0.75AlC2	-0.8871
160	Ti0.75V0.75Nb0.75Mo0.75SiC2	-1.1212	230	V0.75Cr0.75Hf0.75Ta0.75SiC2	-0.8686
161	Ti0.75V0.75Nb0.75Hf0.75AlC2	-0.8125	231	V0.75Zr0.75Nb0.75Mo0.75AlC2	-1.1023
162	Ti0.75V0.75Nb0.75Hf0.75SiC2	-0.8556	232	V0.75Zr0.75Nb0.75Mo0.75SiC2	-1.0854
163	Ti0.75V0.75Nb0.75Ta0.75AlC2	-0.8036	233	V0.75Zr0.75Nb0.75Hf0.75AlC2	-0.8053
164	Ti0.75V0.75Nb0.75Ta0.75SiC2	-0.7979	234	V0.75Zr0.75Nb0.75Hf0.75SiC2	-0.8334
165	Ti0.75V0.75Mo0.75Hf0.75AlC2	-1.1961	235	V0.75Zr0.75Nb0.75Ta0.75AlC2	-0.7537
166	Ti0.75V0.75Mo0.75Hf0.75SiC2	-1.2030	236	V0.75Zr0.75Nb0.75Ta0.75SiC2	-0.7589

167	Ti0.75V0.75Mo0.75Ta0.75AlC2	-1.1622	237	V0.75Zr0.75Mo0.75Hf0.75AlC2	-1.1600
168	Ti0.75V0.75Mo0.75Ta0.75SiC2	-1.1418	238	V0.75Zr0.75Mo0.75Hf0.75SiC2	-1.1571
169	Ti0.75V0.75Hf0.75Ta0.75AlC2	-0.8534	239	V0.75Zr0.75Mo0.75Ta0.75AlC2	-1.0931
170	Ti0.75V0.75Hf0.75Ta0.75SiC2	-0.8798	240	V0.75Zr0.75Mo0.75Ta0.75SiC2	-1.0868
171	Ti0.75Cr0.75Zr0.75Nb0.75AlC2	-0.7375	241	V0.75Zr0.75Hf0.75Ta0.75AlC2	-0.8151
172	Ti0.75Cr0.75Zr0.75Nb0.75SiC2	-0.7446	242	V0.75Zr0.75Hf0.75Ta0.75SiC2	-0.8642
173	Ti0.75Cr0.75Zr0.75Mo0.75AlC2	-1.0914	243	V0.75Nb0.75Mo0.75Hf0.75AlC2	-1.1087
174	Ti0.75Cr0.75Zr0.75Mo0.75SiC2	-1.0893	244	V0.75Nb0.75Mo0.75Hf0.75SiC2	-1.1123
175	Ti0.75Cr0.75Zr0.75Hf0.75AlC2	-0.7784	245	V0.75Nb0.75Mo0.75Ta0.75AlC2	-1.0596
176	Ti0.75Cr0.75Zr0.75Hf0.75SiC2	-0.8236	246	V0.75Nb0.75Mo0.75Ta0.75SiC2	-1.0232
177	Ti0.75Cr0.75Zr0.75Ta0.75AlC2	-0.7525	247	V0.75Nb0.75Hf0.75Ta0.75AlC2	-0.7750
178	Ti0.75Cr0.75Zr0.75Ta0.75SiC2	-0.7626	248	V0.75Nb0.75Hf0.75Ta0.75SiC2	-0.8014
179	Ti0.75Cr0.75Nb0.75Mo0.75AlC2	-1.0835	249	V0.75Mo0.75Hf0.75Ta0.75AlC2	-1.1386
180	Ti0.75Cr0.75Nb0.75Mo0.75SiC2	-1.0231	250	V0.75Mo0.75Hf0.75Ta0.75SiC2	-1.1182
181	Ti0.75Cr0.75Nb0.75Hf0.75AlC2	-0.7672	251	Cr0.75Zr0.75Nb0.75Mo0.75AlC2	-0.9877
182	Ti0.75Cr0.75Nb0.75Hf0.75SiC2	-0.7971	252	Cr0.75Zr0.75Nb0.75Mo0.75SiC2	-0.9989
183	Ti0.75Cr0.75Nb0.75Ta0.75AlC2	-0.7360	253	Cr0.75Zr0.75Nb0.75Hf0.75AlC2	-0.7267
184	Ti0.75Cr0.75Nb0.75Ta0.75SiC2	-0.7218	254	Cr0.75Zr0.75Nb0.75Hf0.75SiC2	-0.7569
185	Ti0.75Cr0.75Mo0.75Hf0.75AlC2	-1.1171	255	Cr0.75Zr0.75Nb0.75Ta0.75AlC2	-0.6721
186	Ti0.75Cr0.75Mo0.75Hf0.75SiC2	-1.1043	256	Cr0.75Zr0.75Nb0.75Ta0.75SiC2	-0.6819
187	Ti0.75Cr0.75Mo0.75Ta0.75AlC2	-1.0791	257	Cr0.75Zr0.75Mo0.75Hf0.75AlC2	-1.0802
188	Ti0.75Cr0.75Mo0.75Ta0.75SiC2	-1.0554	258	Cr0.75Zr0.75Mo0.75Hf0.75SiC2	-1.0680
189	Ti0.75Cr0.75Hf0.75Ta0.75AlC2	-0.7811	259	Cr0.75Zr0.75Mo0.75Ta0.75AlC2	-1.0143
190	Ti0.75Cr0.75Hf0.75Ta0.75SiC2	-0.8051	260	Cr0.75Zr0.75Mo0.75Ta0.75SiC2	-1.0112
191	Ti0.75Zr0.75Nb0.75Mo0.75AlC2	-0.9873	261	Cr0.75Zr0.75Hf0.75Ta0.75AlC2	-0.7448
192	Ti0.75Zr0.75Nb0.75Mo0.75SiC2	-0.9900	262	Cr0.75Zr0.75Hf0.75Ta0.75SiC2	-0.7799
193	Ti0.75Zr0.75Nb0.75Hf0.75AlC2	-0.6917	263	Cr0.75Nb0.75Mo0.75Hf0.75AlC2	-1.0475
194	Ti0.75Zr0.75Nb0.75Hf0.75SiC2	-0.7444	264	Cr0.75Nb0.75Mo0.75Hf0.75SiC2	-1.0272
195	Ti0.75Zr0.75Nb0.75Ta0.75AlC2	-0.6474	265	Cr0.75Nb0.75Mo0.75Ta0.75AlC2	-0.9724
196	Ti0.75Zr0.75Nb0.75Ta0.75SiC2	-0.6745	266	Cr0.75Nb0.75Mo0.75Ta0.75SiC2	-0.9499
197	Ti0.75Zr0.75Mo0.75Hf0.75AlC2	-1.0464	267	Cr0.75Nb0.75Hf0.75Ta0.75AlC2	-0.7064

198	Ti0.75Zr0.75Mo0.75Hf0.75SiC2	-1.0751	268	Cr0.75Nb0.75Hf0.75Ta0.75SiC2	-0.7259
199	Ti0.75Zr0.75Mo0.75Ta0.75AlC2	-1.0114	269	Cr0.75Mo0.75Hf0.75Ta0.75AlC2	-1.0526
200	Ti0.75Zr0.75Mo0.75Ta0.75SiC2	-1.0071	270	Cr0.75Mo0.75Hf0.75Ta0.75SiC2	-1.0464
201	Ti0.75Zr0.75Hf0.75Ta0.75AlC2	-0.7073	271	Zr0.75Nb0.75Mo0.75Hf0.75AlC2	-1.0045
202	Ti0.75Zr0.75Hf0.75Ta0.75SiC2	-0.7633	272	Zr0.75Nb0.75Mo0.75Hf0.75SiC2	-0.9923
203	Ti0.75Nb0.75Mo0.75Hf0.75AlC2	-1.0214	273	Zr0.75Nb0.75Mo0.75Ta0.75AlC2	-0.9253
204	Ti0.75Nb0.75Mo0.75Hf0.75SiC2	-1.0189	274	Zr0.75Nb0.75Mo0.75Ta0.75SiC2	-0.9131
205	Ti0.75Nb0.75Mo0.75Ta0.75AlC2	-0.9691	275	Zr0.75Nb0.75Hf0.75Ta0.75AlC2	-0.6611
206	Ti0.75Nb0.75Mo0.75Ta0.75SiC2	-0.9420	276	Zr0.75Nb0.75Hf0.75Ta0.75SiC2	-0.6904
207	Ti0.75Nb0.75Hf0.75Ta0.75AlC2	-0.6780	277	Zr0.75Mo0.75Hf0.75Ta0.75AlC2	-1.0204
208	Ti0.75Nb0.75Hf0.75Ta0.75SiC2	-0.6950	278	Zr0.75Mo0.75Hf0.75Ta0.75SiC2	-1.0284
209	Ti0.75Mo0.75Hf0.75Ta0.75AlC2	-1.0389	279	Nb0.75Mo0.75Hf0.75Ta0.75AlC2	-0.9711
210	Ti0.75Mo0.75Hf0.75Ta0.75SiC2	-1.0336	280	Nb0.75Mo0.75Hf0.75Ta0.75SiC2	-0.9399

Table S3. 5_M_2AC HE-MAX candidates (Index 281–392; N = 112) with compositions and formation energies (Ef, eV/atom) used for thermodynamic stability screening.

Index Number	Formula	Formation Energy (eV/atom)	Index Number	Formula	Formation Energy (eV/atom)
281	Ti0.6V0.6Cr0.6Zr0.6Nb0.6AlC2	-0.83738	337	Ti0.6Cr0.6Nb0.6Hf0.6Ta0.6AlC2	-0.72769
282	Ti0.6V0.6Cr0.6Zr0.6Nb0.6SiC2	-0.85851	338	Ti0.6Cr0.6Nb0.6Hf0.6Ta0.6SiC2	-0.74906
283	Ti0.6V0.6Cr0.6Zr0.6Mo0.6AlC2	-1.12188	339	Ti0.6Cr0.6Mo0.6Hf0.6Ta0.6AlC2	-1.00891
284	Ti0.6V0.6Cr0.6Zr0.6Mo0.6SiC2	-1.10898	340	Ti0.6Cr0.6Mo0.6Hf0.6Ta0.6SiC2	-1.01064
285	Ti0.6V0.6Cr0.6Zr0.6Hf0.6AlC2	-0.85522	341	Ti0.6Zr0.6Nb0.6Mo0.6Hf0.6AlC2	-0.95285
286	Ti0.6V0.6Cr0.6Zr0.6Hf0.6SiC2	-0.89647	342	Ti0.6Zr0.6Nb0.6Mo0.6Hf0.6SiC2	-0.96131
287	Ti0.6V0.6Cr0.6Zr0.6Ta0.6AlC2	-0.85501	343	Ti0.6Zr0.6Nb0.6Mo0.6Ta0.6AlC2	-0.90806
288	Ti0.6V0.6Cr0.6Zr0.6Ta0.6SiC2	-0.86112	344	Ti0.6Zr0.6Nb0.6Mo0.6Ta0.6SiC2	-0.90296
289	Ti0.6V0.6Cr0.6Nb0.6Mo0.6AlC2	-1.10903	345	Ti0.6Zr0.6Nb0.6Hf0.6Ta0.6AlC2	-0.67804
290	Ti0.6V0.6Cr0.6Nb0.6Mo0.6SiC2	-1.07587	346	Ti0.6Zr0.6Nb0.6Hf0.6Ta0.6SiC2	-0.71413
291	Ti0.6V0.6Cr0.6Nb0.6Hf0.6AlC2	-0.85505	347	Ti0.6Zr0.6Mo0.6Hf0.6Ta0.6AlC2	-0.95717
292	Ti0.6V0.6Cr0.6Nb0.6Hf0.6SiC2	-0.88238	348	Ti0.6Zr0.6Mo0.6Hf0.6Ta0.6SiC2	-0.96999
293	Ti0.6V0.6Cr0.6Nb0.6Ta0.6AlC2	-0.84119	349	Ti0.6Nb0.6Mo0.6Hf0.6Ta0.6AlC2	-0.93942
294	Ti0.6V0.6Cr0.6Nb0.6Ta0.6SiC2	-0.84558	350	Ti0.6Nb0.6Mo0.6Hf0.6Ta0.6SiC2	-0.92240
295	Ti0.6V0.6Cr0.6Mo0.6Hf0.6AlC2	-1.15646	351	V0.6Cr0.6Zr0.6Nb0.6Mo0.6AlC2	-1.05896
296	Ti0.6V0.6Cr0.6Mo0.6Hf0.6SiC2	-1.14678	352	V0.6Cr0.6Zr0.6Nb0.6Mo0.6SiC2	-1.04985
297	Ti0.6V0.6Cr0.6Mo0.6Ta0.6AlC2	-1.12306	353	V0.6Cr0.6Zr0.6Nb0.6Hf0.6AlC2	-0.81275
298	Ti0.6V0.6Cr0.6Mo0.6Ta0.6SiC2	-1.11332	354	V0.6Cr0.6Zr0.6Nb0.6Hf0.6SiC2	-0.83464
299	Ti0.6V0.6Cr0.6Hf0.6Ta0.6AlC2	-0.87606	355	V0.6Cr0.6Zr0.6Nb0.6Ta0.6AlC2	-0.79618
300	Ti0.6V0.6Cr0.6Hf0.6Ta0.6SiC2	-0.89219	356	V0.6Cr0.6Zr0.6Nb0.6Ta0.6SiC2	-0.78813
301	Ti0.6V0.6Zr0.6Nb0.6Mo0.6AlC2	-1.04071	357	V0.6Cr0.6Zr0.6Mo0.6Hf0.6AlC2	-1.08888
302	Ti0.6V0.6Zr0.6Nb0.6Mo0.6SiC2	-1.04325	358	V0.6Cr0.6Zr0.6Mo0.6Hf0.6SiC2	-1.12387
303	Ti0.6V0.6Zr0.6Nb0.6Hf0.6AlC2	-0.78671	359	V0.6Cr0.6Zr0.6Mo0.6Ta0.6AlC2	-1.07165
304	Ti0.6V0.6Zr0.6Nb0.6Hf0.6SiC2	-0.82661	360	V0.6Cr0.6Zr0.6Mo0.6Ta0.6SiC2	-1.05259
305	Ti0.6V0.6Zr0.6Nb0.6Ta0.6AlC2	-0.77198	361	V0.6Cr0.6Zr0.6Hf0.6Ta0.6AlC2	-0.83751
306	Ti0.6V0.6Zr0.6Nb0.6Ta0.6SiC2	-0.78308	362	V0.6Cr0.6Zr0.6Hf0.6Ta0.6SiC2	-0.84508
307	Ti0.6V0.6Zr0.6Mo0.6Hf0.6AlC2	-1.07291	363	V0.6Cr0.6Nb0.6Mo0.6Hf0.6AlC2	-1.08296

308	Ti0.6V0.6Zr0.6Mo0.6Hf0.6SiC2	-1.08670	364	V0.6Cr0.6Nb0.6Mo0.6Hf0.6SiC2	-1.05586
309	Ti0.6V0.6Zr0.6Mo0.6Ta0.6AlC2	-1.04975	365	V0.6Cr0.6Nb0.6Mo0.6Ta0.6AlC2	-1.05071
310	Ti0.6V0.6Zr0.6Mo0.6Ta0.6SiC2	-1.05410	366	V0.6Cr0.6Nb0.6Mo0.6Ta0.6SiC2	-1.01861
311	Ti0.6V0.6Zr0.6Hf0.6Ta0.6AlC2	-0.79943	367	V0.6Cr0.6Nb0.6Hf0.6Ta0.6AlC2	-0.81832
312	Ti0.6V0.6Zr0.6Hf0.6Ta0.6SiC2	-0.84345	368	V0.6Cr0.6Nb0.6Hf0.6Ta0.6SiC2	-0.79261
313	Ti0.6V0.6Nb0.6Mo0.6Hf0.6AlC2	-1.06500	369	V0.6Cr0.6Mo0.6Hf0.6Ta0.6AlC2	-1.07893
314	Ti0.6V0.6Nb0.6Mo0.6Hf0.6SiC2	-1.06411	370	V0.6Cr0.6Mo0.6Hf0.6Ta0.6SiC2	-1.07297
315	Ti0.6V0.6Nb0.6Mo0.6Ta0.6AlC2	-1.03479	371	V0.6Zr0.6Nb0.6Mo0.6Hf0.6AlC2	-1.02113
316	Ti0.6V0.6Nb0.6Mo0.6Ta0.6SiC2	-1.00768	372	V0.6Zr0.6Nb0.6Mo0.6Hf0.6SiC2	-1.03264
317	Ti0.6V0.6Nb0.6Hf0.6Ta0.6AlC2	-0.78446	373	V0.6Zr0.6Nb0.6Mo0.6Ta0.6AlC2	-0.99930
318	Ti0.6V0.6Nb0.6Hf0.6Ta0.6SiC2	-0.80088	374	V0.6Zr0.6Nb0.6Mo0.6Ta0.6SiC2	-0.98275
319	Ti0.6V0.6Mo0.6Hf0.6Ta0.6AlC2	-1.08425	375	V0.6Zr0.6Nb0.6Hf0.6Ta0.6AlC2	-0.75422
320	Ti0.6V0.6Mo0.6Hf0.6Ta0.6SiC2	-1.08268	376	V0.6Zr0.6Nb0.6Hf0.6Ta0.6SiC2	-0.78686
321	Ti0.6Cr0.6Zr0.6Nb0.6Mo0.6AlC2	-0.95721	377	V0.6Zr0.6Mo0.6Hf0.6Ta0.6AlC2	-1.03592
322	Ti0.6Cr0.6Zr0.6Nb0.6Mo0.6SiC2	-0.97408	378	V0.6Zr0.6Mo0.6Hf0.6Ta0.6SiC2	-1.05680
323	Ti0.6Cr0.6Zr0.6Nb0.6Hf0.6AlC2	-0.73466	379	V0.6Nb0.6Mo0.6Hf0.6Ta0.6AlC2	-1.02351
324	Ti0.6Cr0.6Zr0.6Nb0.6Hf0.6SiC2	-0.77289	380	V0.6Nb0.6Mo0.6Hf0.6Ta0.6SiC2	-1.00240
325	Ti0.6Cr0.6Zr0.6Nb0.6Ta0.6AlC2	-0.70334	381	Cr0.6Zr0.6Nb0.6Mo0.6Hf0.6AlC2	-0.97784
326	Ti0.6Cr0.6Zr0.6Nb0.6Ta0.6SiC2	-0.72651	382	Cr0.6Zr0.6Nb0.6Mo0.6Hf0.6SiC2	-0.96576
327	Ti0.6Cr0.6Zr0.6Mo0.6Hf0.6AlC2	-1.03036	383	Cr0.6Zr0.6Nb0.6Mo0.6Ta0.6AlC2	-0.92298
328	Ti0.6Cr0.6Zr0.6Mo0.6Hf0.6SiC2	-1.03505	384	Cr0.6Zr0.6Nb0.6Mo0.6Ta0.6SiC2	-0.91967
329	Ti0.6Cr0.6Zr0.6Mo0.6Ta0.6AlC2	-0.99263	385	Cr0.6Zr0.6Nb0.6Hf0.6Ta0.6AlC2	-0.71282
330	Ti0.6Cr0.6Zr0.6Mo0.6Ta0.6SiC2	-0.99040	386	Cr0.6Zr0.6Nb0.6Hf0.6Ta0.6SiC2	-0.72204
331	Ti0.6Cr0.6Zr0.6Hf0.6Ta0.6AlC2	-0.75481	387	Cr0.6Zr0.6Mo0.6Hf0.6Ta0.6AlC2	-0.98797
332	Ti0.6Cr0.6Zr0.6Hf0.6Ta0.6SiC2	-0.78488	388	Cr0.6Zr0.6Mo0.6Hf0.6Ta0.6SiC2	-0.98638
333	Ti0.6Cr0.6Nb0.6Mo0.6Hf0.6AlC2	-1.00590	389	Cr0.6Nb0.6Mo0.6Hf0.6Ta0.6AlC2	-0.97837
334	Ti0.6Cr0.6Nb0.6Mo0.6Hf0.6SiC2	-0.99462	390	Cr0.6Nb0.6Mo0.6Hf0.6Ta0.6SiC2	-0.94041
335	Ti0.6Cr0.6Nb0.6Mo0.6Ta0.6AlC2	-0.98037	391	Zr0.6Nb0.6Mo0.6Hf0.6Ta0.6AlC2	-0.91582
336	Ti0.6Cr0.6Nb0.6Mo0.6Ta0.6SiC2	-0.96377	392	Zr0.6Nb0.6Mo0.6Hf0.6Ta0.6SiC2	-0.92076

Table S4. 5_M_3AC_2 HE-MAX candidates (Index 393–504; N = 112) with compositions and formation energies (Ef, eV/atom) used for thermodynamic stability screening.

Index Number	Formula	Formation Energy (eV/atom)	Index Number	Formula	Formation Energy (eV/atom)
393	Ti0.4V0.4Cr0.4Zr0.4Nb0.4AlC	-0.83405	449	Ti0.4Cr0.4Nb0.4Hf0.4Ta0.4AlC	-0.69766
394	Ti0.4V0.4Cr0.4Zr0.4Nb0.4SiC	-0.87658	450	Ti0.4Cr0.4Nb0.4Hf0.4Ta0.4SiC	-0.73458
395	Ti0.4V0.4Cr0.4Zr0.4Mo0.4AlC	-1.14234	451	Ti0.4Cr0.4Mo0.4Hf0.4Ta0.4AlC	-1.00508
396	Ti0.4V0.4Cr0.4Zr0.4Mo0.4SiC	-1.16471	452	Ti0.4Cr0.4Mo0.4Hf0.4Ta0.4SiC	-1.01396
397	Ti0.4V0.4Cr0.4Zr0.4Hf0.4AlC	-0.85531	453	Ti0.4Zr0.4Nb0.4Mo0.4Hf0.4AlC	-0.91724
398	Ti0.4V0.4Cr0.4Zr0.4Hf0.4SiC	-0.90555	454	Ti0.4Zr0.4Nb0.4Mo0.4Hf0.4SiC	-0.96352
399	Ti0.4V0.4Cr0.4Zr0.4Ta0.4AlC	-0.85426	455	Ti0.4Zr0.4Nb0.4Mo0.4Ta0.4AlC	-0.88699
400	Ti0.4V0.4Cr0.4Zr0.4Ta0.4SiC	-0.85727	456	Ti0.4Zr0.4Nb0.4Mo0.4Ta0.4SiC	-0.91635
401	Ti0.4V0.4Cr0.4Nb0.4Mo0.4AlC	-1.13003	457	Ti0.4Zr0.4Nb0.4Hf0.4Ta0.4AlC	-0.62705
402	Ti0.4V0.4Cr0.4Nb0.4Mo0.4SiC	-1.13004	458	Ti0.4Zr0.4Nb0.4Hf0.4Ta0.4SiC	-0.69405
403	Ti0.4V0.4Cr0.4Nb0.4Hf0.4AlC	-0.85003	459	Ti0.4Zr0.4Mo0.4Hf0.4Ta0.4AlC	-0.92127
404	Ti0.4V0.4Cr0.4Nb0.4Hf0.4SiC	-0.87939	460	Ti0.4Zr0.4Mo0.4Hf0.4Ta0.4SiC	-0.96963
405	Ti0.4V0.4Cr0.4Nb0.4Ta0.4AlC	-0.82826	461	Ti0.4Nb0.4Mo0.4Hf0.4Ta0.4AlC	-0.89987
406	Ti0.4V0.4Cr0.4Nb0.4Ta0.4SiC	-0.83519	462	Ti0.4Nb0.4Mo0.4Hf0.4Ta0.4SiC	-0.92328
407	Ti0.4V0.4Cr0.4Mo0.4Hf0.4AlC	-1.16051	463	V0.4Cr0.4Zr0.4Nb0.4Mo0.4AlC	-1.08588
408	Ti0.4V0.4Cr0.4Mo0.4Hf0.4SiC	-1.17374	464	V0.4Cr0.4Zr0.4Nb0.4Mo0.4SiC	-1.11317
409	Ti0.4V0.4Cr0.4Mo0.4Ta0.4AlC	-1.14188	465	V0.4Cr0.4Zr0.4Nb0.4Hf0.4AlC	-0.81770
410	Ti0.4V0.4Cr0.4Mo0.4Ta0.4SiC	-1.13531	466	V0.4Cr0.4Zr0.4Nb0.4Hf0.4SiC	-0.84305
411	Ti0.4V0.4Cr0.4Hf0.4Ta0.4AlC	-0.86279	467	V0.4Cr0.4Zr0.4Nb0.4Ta0.4AlC	-0.80244
412	Ti0.4V0.4Cr0.4Hf0.4Ta0.4SiC	-0.89693	468	V0.4Cr0.4Zr0.4Nb0.4Ta0.4SiC	-0.80173
413	Ti0.4V0.4Zr0.4Nb0.4Mo0.4AlC	-1.02705	469	V0.4Cr0.4Zr0.4Mo0.4Hf0.4AlC	-1.12615
414	Ti0.4V0.4Zr0.4Nb0.4Mo0.4SiC	-1.04877	470	V0.4Cr0.4Zr0.4Mo0.4Hf0.4SiC	-1.14092
415	Ti0.4V0.4Zr0.4Nb0.4Hf0.4AlC	-0.75876	471	V0.4Cr0.4Zr0.4Mo0.4Ta0.4AlC	-1.10550
416	Ti0.4V0.4Zr0.4Nb0.4Hf0.4SiC	-0.82351	472	V0.4Cr0.4Zr0.4Mo0.4Ta0.4SiC	-1.08894
417	Ti0.4V0.4Zr0.4Nb0.4Ta0.4AlC	-0.73879	473	V0.4Cr0.4Zr0.4Hf0.4Ta0.4AlC	-0.82374
418	Ti0.4V0.4Zr0.4Nb0.4Ta0.4SiC	-0.77732	474	V0.4Cr0.4Zr0.4Hf0.4Ta0.4SiC	-0.84431
419	Ti0.4V0.4Zr0.4Mo0.4Hf0.4AlC	-1.06752	475	V0.4Cr0.4Nb0.4Mo0.4Hf0.4AlC	-1.10548

420	Ti0.4V0.4Zr0.4Mo0.4Hf0.4SiC	-1.10742	476	V0.4Cr0.4Nb0.4Mo0.4Hf0.4SiC	-1.10284
421	Ti0.4V0.4Zr0.4Mo0.4Ta0.4AlC	-1.03649	477	V0.4Cr0.4Nb0.4Mo0.4Ta0.4AlC	-1.07106
422	Ti0.4V0.4Zr0.4Mo0.4Ta0.4SiC	-1.06065	478	V0.4Cr0.4Nb0.4Mo0.4Ta0.4SiC	-1.07449
423	Ti0.4V0.4Zr0.4Hf0.4Ta0.4AlC	-0.76378	479	V0.4Cr0.4Nb0.4Hf0.4Ta0.4AlC	-0.81355
424	Ti0.4V0.4Zr0.4Hf0.4Ta0.4SiC	-0.83443	480	V0.4Cr0.4Nb0.4Hf0.4Ta0.4SiC	-0.79507
425	Ti0.4V0.4Nb0.4Mo0.4Hf0.4AlC	-1.04357	481	V0.4Cr0.4Mo0.4Hf0.4Ta0.4AlC	-1.11122
426	Ti0.4V0.4Nb0.4Mo0.4Hf0.4SiC	-1.07517	482	V0.4Cr0.4Mo0.4Hf0.4Ta0.4SiC	-1.10623
427	Ti0.4V0.4Nb0.4Mo0.4Ta0.4AlC	-1.02336	483	V0.4Zr0.4Nb0.4Mo0.4Hf0.4AlC	-1.01392
428	Ti0.4V0.4Nb0.4Mo0.4Ta0.4SiC	-1.02682	484	V0.4Zr0.4Nb0.4Mo0.4Hf0.4SiC	-1.04945
429	Ti0.4V0.4Nb0.4Hf0.4Ta0.4AlC	-0.75284	485	V0.4Zr0.4Nb0.4Mo0.4Ta0.4AlC	-0.98331
430	Ti0.4V0.4Nb0.4Hf0.4Ta0.4SiC	-0.80088	486	V0.4Zr0.4Nb0.4Mo0.4Ta0.4SiC	-1.00673
431	Ti0.4V0.4Mo0.4Hf0.4Ta0.4AlC	-1.05318	487	V0.4Zr0.4Nb0.4Hf0.4Ta0.4AlC	-0.72938
432	Ti0.4V0.4Mo0.4Hf0.4Ta0.4SiC	-1.08294	488	V0.4Zr0.4Nb0.4Hf0.4Ta0.4SiC	-0.77999
433	Ti0.4Cr0.4Zr0.4Nb0.4Mo0.4AlC	-0.97910	489	V0.4Zr0.4Mo0.4Hf0.4Ta0.4AlC	-1.02575
434	Ti0.4Cr0.4Zr0.4Nb0.4Mo0.4SiC	-1.00309	490	V0.4Zr0.4Mo0.4Hf0.4Ta0.4SiC	-1.06131
435	Ti0.4Cr0.4Zr0.4Nb0.4Hf0.4AlC	-0.69497	491	V0.4Nb0.4Mo0.4Hf0.4Ta0.4AlC	-0.99977
436	Ti0.4Cr0.4Zr0.4Nb0.4Hf0.4SiC	-0.77159	492	V0.4Nb0.4Mo0.4Hf0.4Ta0.4SiC	-1.01677
437	Ti0.4Cr0.4Zr0.4Nb0.4Ta0.4AlC	-0.67992	493	Cr0.4Zr0.4Nb0.4Mo0.4Hf0.4AlC	-0.96428
438	Ti0.4Cr0.4Zr0.4Nb0.4Ta0.4SiC	-0.71993	494	Cr0.4Zr0.4Nb0.4Mo0.4Hf0.4SiC	-1.01014
439	Ti0.4Cr0.4Zr0.4Mo0.4Hf0.4AlC	-1.00391	495	Cr0.4Zr0.4Nb0.4Mo0.4Ta0.4AlC	-0.92937
440	Ti0.4Cr0.4Zr0.4Mo0.4Hf0.4SiC	-1.05579	496	Cr0.4Zr0.4Nb0.4Mo0.4Ta0.4SiC	-0.94022
441	Ti0.4Cr0.4Zr0.4Mo0.4Ta0.4AlC	-0.98287	497	Cr0.4Zr0.4Nb0.4Hf0.4Ta0.4AlC	-0.67438
442	Ti0.4Cr0.4Zr0.4Mo0.4Ta0.4SiC	-1.00790	498	Cr0.4Zr0.4Nb0.4Hf0.4Ta0.4SiC	-0.70694
443	Ti0.4Cr0.4Zr0.4Hf0.4Ta0.4AlC	-0.71564	499	Cr0.4Zr0.4Mo0.4Hf0.4Ta0.4AlC	-0.97129
444	Ti0.4Cr0.4Zr0.4Hf0.4Ta0.4SiC	-0.77149	500	Cr0.4Zr0.4Mo0.4Hf0.4Ta0.4SiC	-0.99421
445	Ti0.4Cr0.4Nb0.4Mo0.4Hf0.4AlC	-0.99420	501	Cr0.4Nb0.4Mo0.4Hf0.4Ta0.4AlC	-0.94551
446	Ti0.4Cr0.4Nb0.4Mo0.4Hf0.4SiC	-1.01519	502	Cr0.4Nb0.4Mo0.4Hf0.4Ta0.4SiC	-0.95165
447	Ti0.4Cr0.4Nb0.4Mo0.4Ta0.4AlC	-0.96978	503	Zr0.4Nb0.4Mo0.4Hf0.4Ta0.4AlC	-0.87877
448	Ti0.4Cr0.4Nb0.4Mo0.4Ta0.4SiC	-0.96689	504	Zr0.4Nb0.4Mo0.4Hf0.4Ta0.4SiC	-0.91224

ESI 2. At In the initial clustering stage for selecting representative compositions, various evaluation metrics Yellowbrick Elbow, manual inertia calculation, and silhouette score were employed to determine the optimal number of clusters (k) for K-Means based clustering. However, these methods did not yield a consistent conclusion regarding the optimal k value.

First, the distortion score from the Yellowbrick Elbow method suggested an elbow at $k = 4$. Nonetheless, the distortion values continued to decrease gradually beyond this point, indicating that a distinct elbow was not clearly observable. Similarly, the manually calculated inertia values (within-cluster sum of squares, WCSS) showed a continuous decrease as k increased, failing to meet the typical elbow criterion of a sharp decline followed by a plateau. This suggests that the data exhibit structurally complex characteristics with ambiguous boundaries between clusters.

In the silhouette score analysis, the highest score (≈ 0.3232) was observed at $k = 10$. However, the overall silhouette values remained within a low range of 0.25–0.32. Since a silhouette score above 0.5 is generally considered indicative of well-separated clusters, the consistently low scores in this dataset imply limited reliability of clustering quality. This reflects the continuous and high-dimensional nature of the compositional space rather than the presence of discrete cluster boundaries.

Consequently, instead of relying on a single clustering metric or a fixed k value, an ensemble clustering approach using multiple algorithms was adopted as a more robust and reliable strategy to represent complex compositional landscapes like those studied in this work.

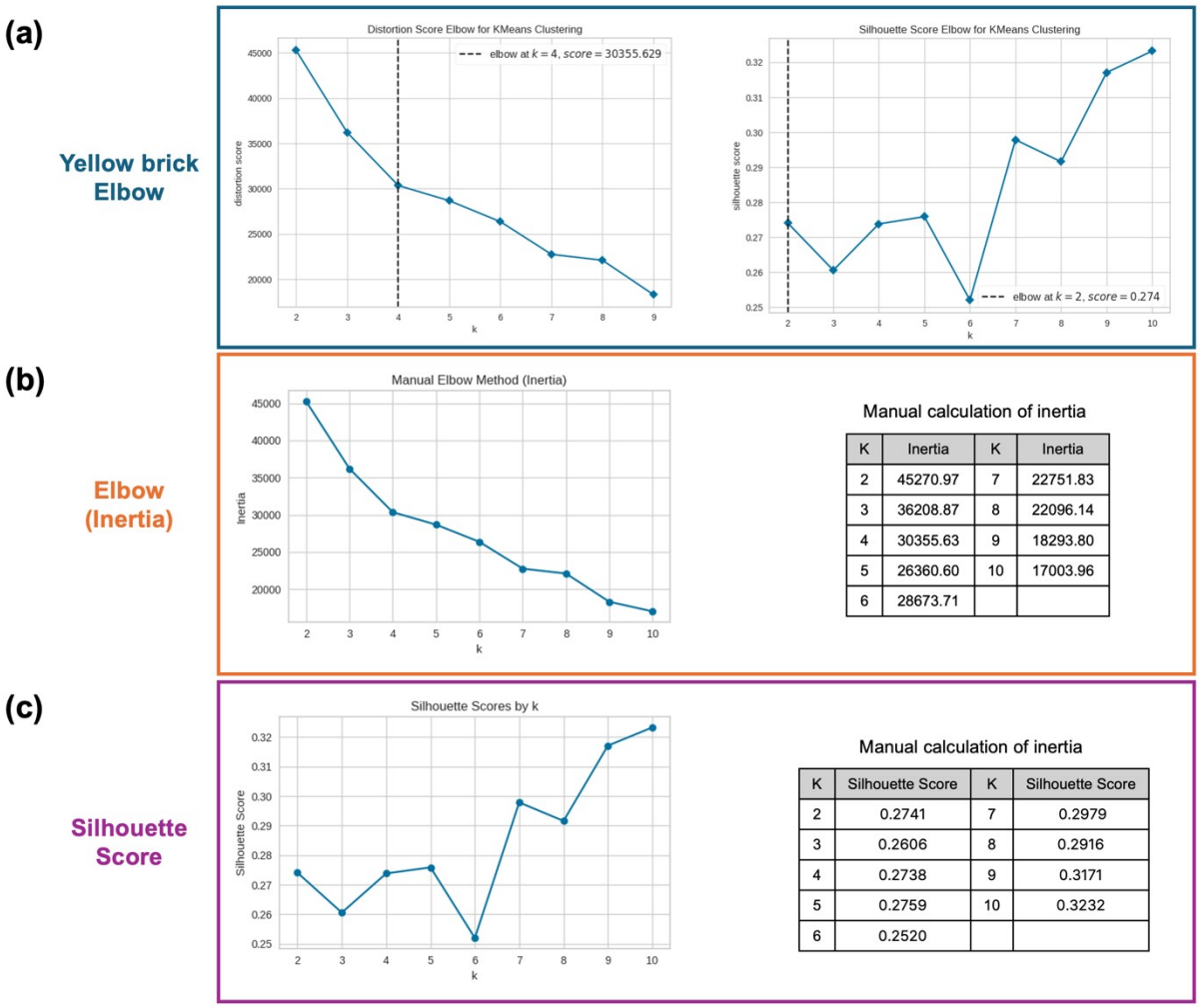

K	Inertia	K	Inertia
2	45270.97	7	22751.83
3	36208.87	8	22096.14
4	30355.63	9	18293.80
5	26360.60	10	17003.96
6	28673.71		

K	Silhouette Score	K	Silhouette Score
2	0.2741	7	0.2979
3	0.2606	8	0.2916
4	0.2738	9	0.3171
5	0.2759	10	0.3232
6	0.2520		

Figure S1. Number Comparison of different methods for determining the optimal number of clusters (k) in K-Means clustering. (a) Yellow brick Elbow plots for distortion and silhouette score. (b) Manual Elbow method using inertia (WCSS). (c) Silhouette scores by k. No consistent or clear k value was identified across methods, indicating the absence of distinct cluster boundaries in the dataset.

ESI 3. At each iteration, only the compositions selected through clustering were used for fine-tuning, while the remaining data served as the test set to evaluate the model's generalization performance. This approach enables continuous assessment of how effectively the model extrapolates the learned information across the entire compositional space.

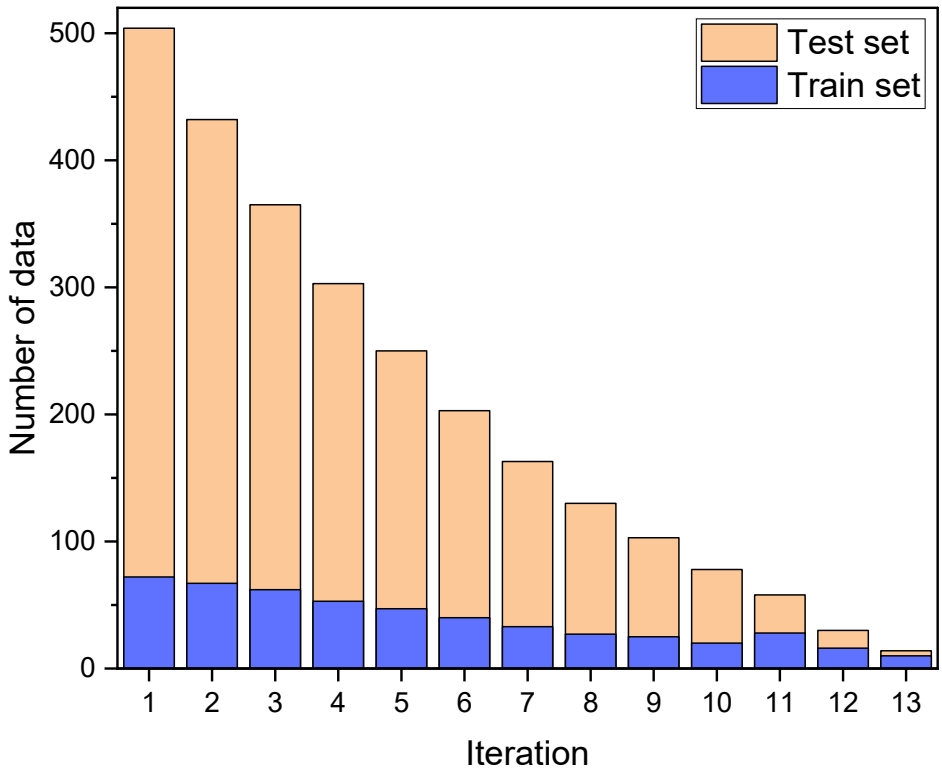

Figure S2. Number of train and test data used at each fine-tuning iteration. At every step, only the clustering-selected representative compositions were used for model training (blue), while the remaining compositions served as the test set (orange) to evaluate generalization performance across the unexplored compositional space.

ESI 4. As shown in the training progress logs from the 1st to the 12th fine-tuning iterations, the MAE values for all target properties energy (e_MAE), force (f_MAE), stress (s_MAE), and magnetic moment (m_MAE) generally show a downward trend as training progresses. This indicates that the model continues to learn a more accurate representation of the underlying potential energy surface through iterative fine-tuning. However, a few irregularities are observed. for example, in the 2nd iteration, a notable spike appears in the early phase of training, suggesting instability or noise in the optimization process. Similarly, the 4th and 10th iterations display intermittent fluctuations in MAE, particularly in the stress predictions (s_MAE). Despite these anomalies, the overall training behavior remains consistent across iterations, with each stage contributing to lower and more stable MAE values. This progressive refinement supports the robustness and convergence of the fine-tuning process.

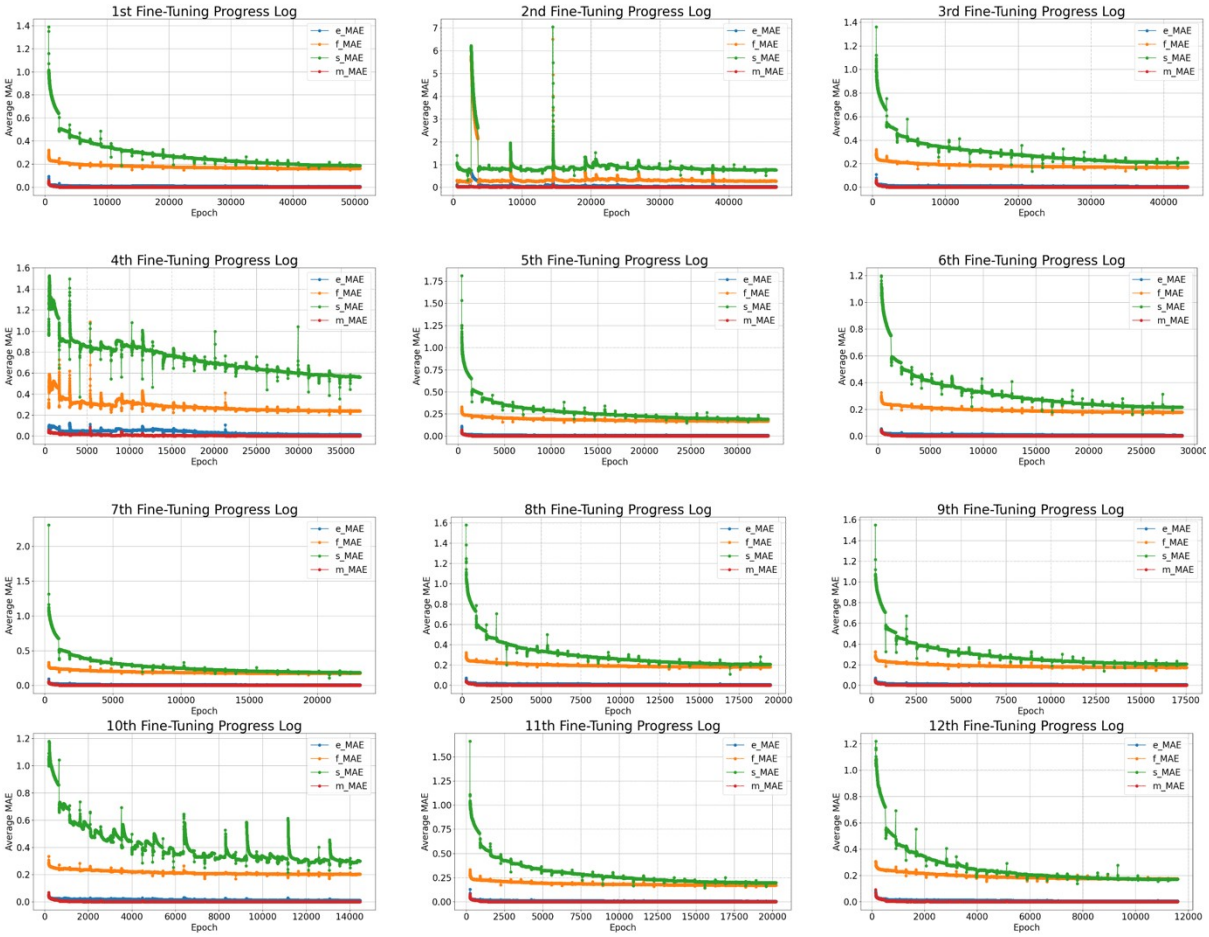

Figure S3. Average MAE values over training epochs from Iteration 1 to 12.

ESI 5. MAE and R^2 values across iterations for Methods 1 to 4.

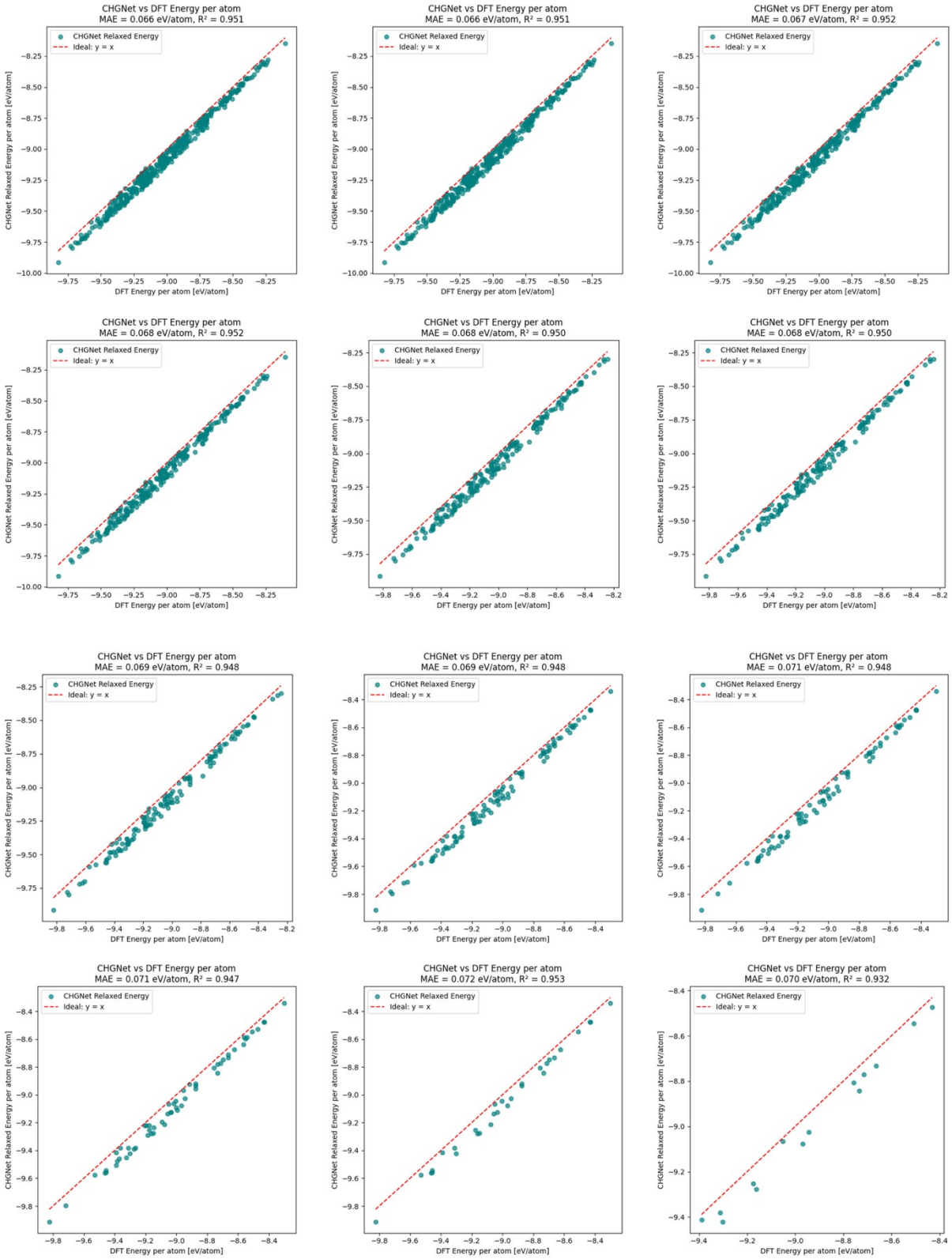

Figure S4. MAE and R^2 values after each iteration from 1 to 12 for Method 1.

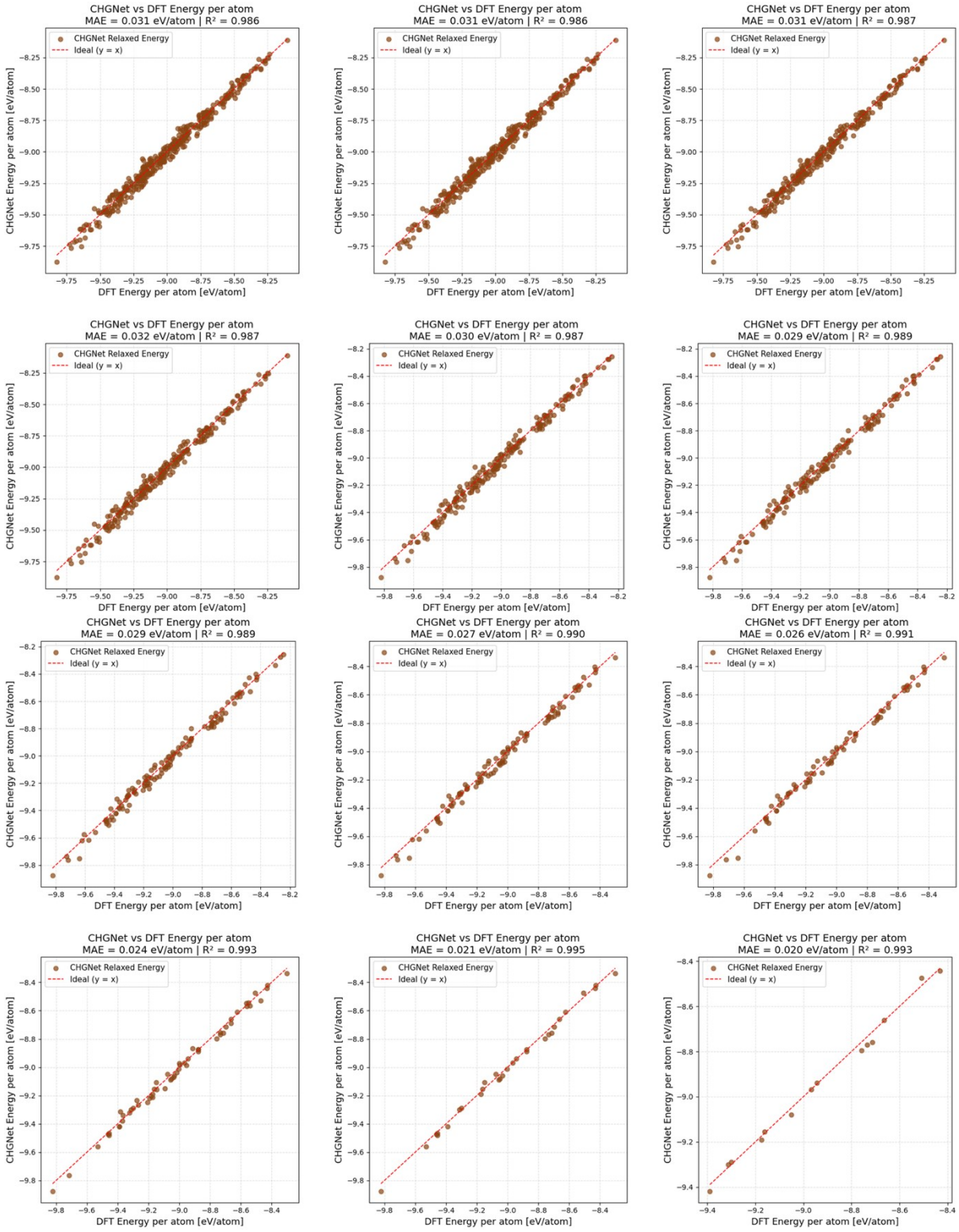

Figure S5. MAE and R^2 values after each iteration from 1 to 12 for Method 2.

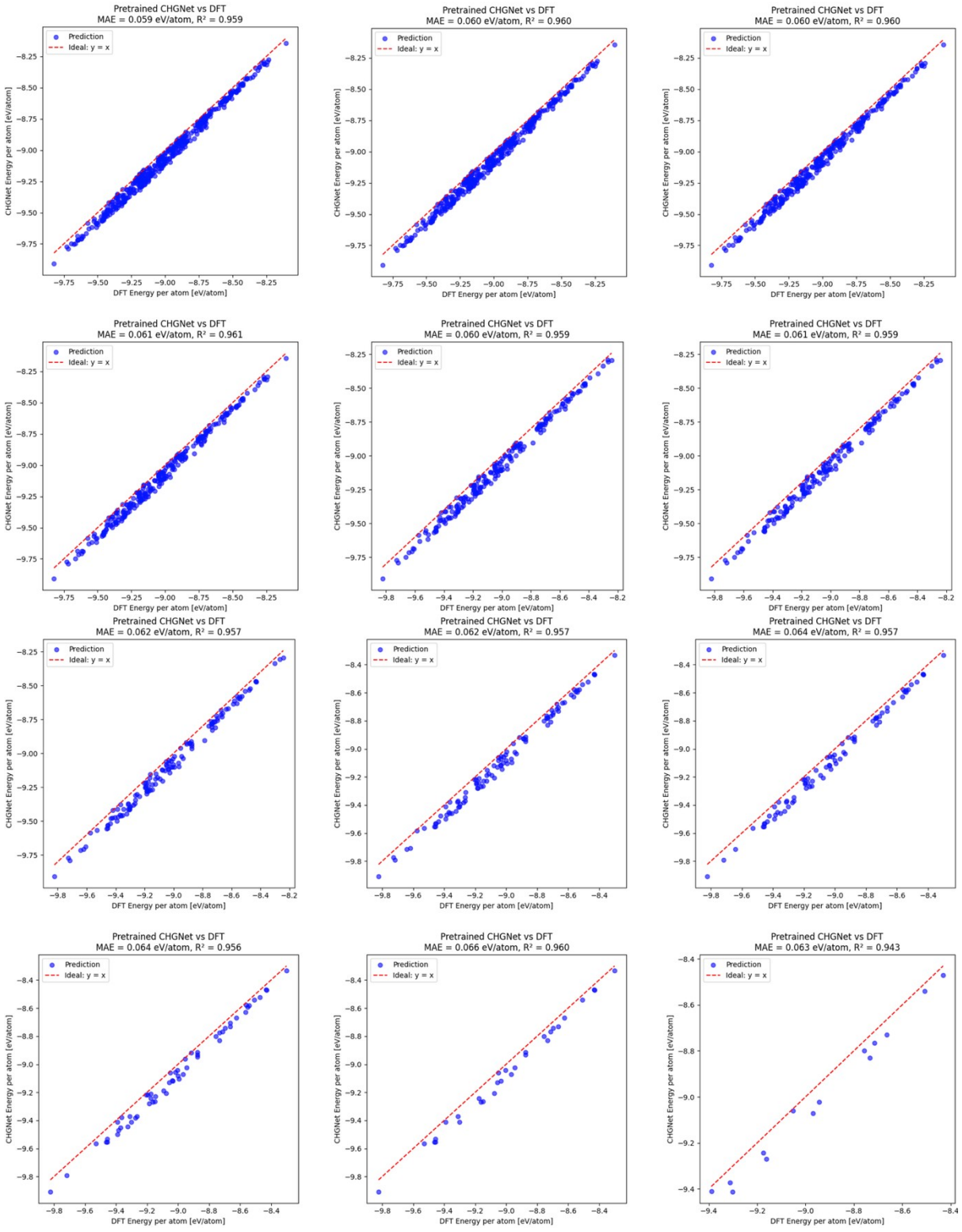

Figure S6. MAE and R^2 values after each iteration from 1 to 12 for Method3.

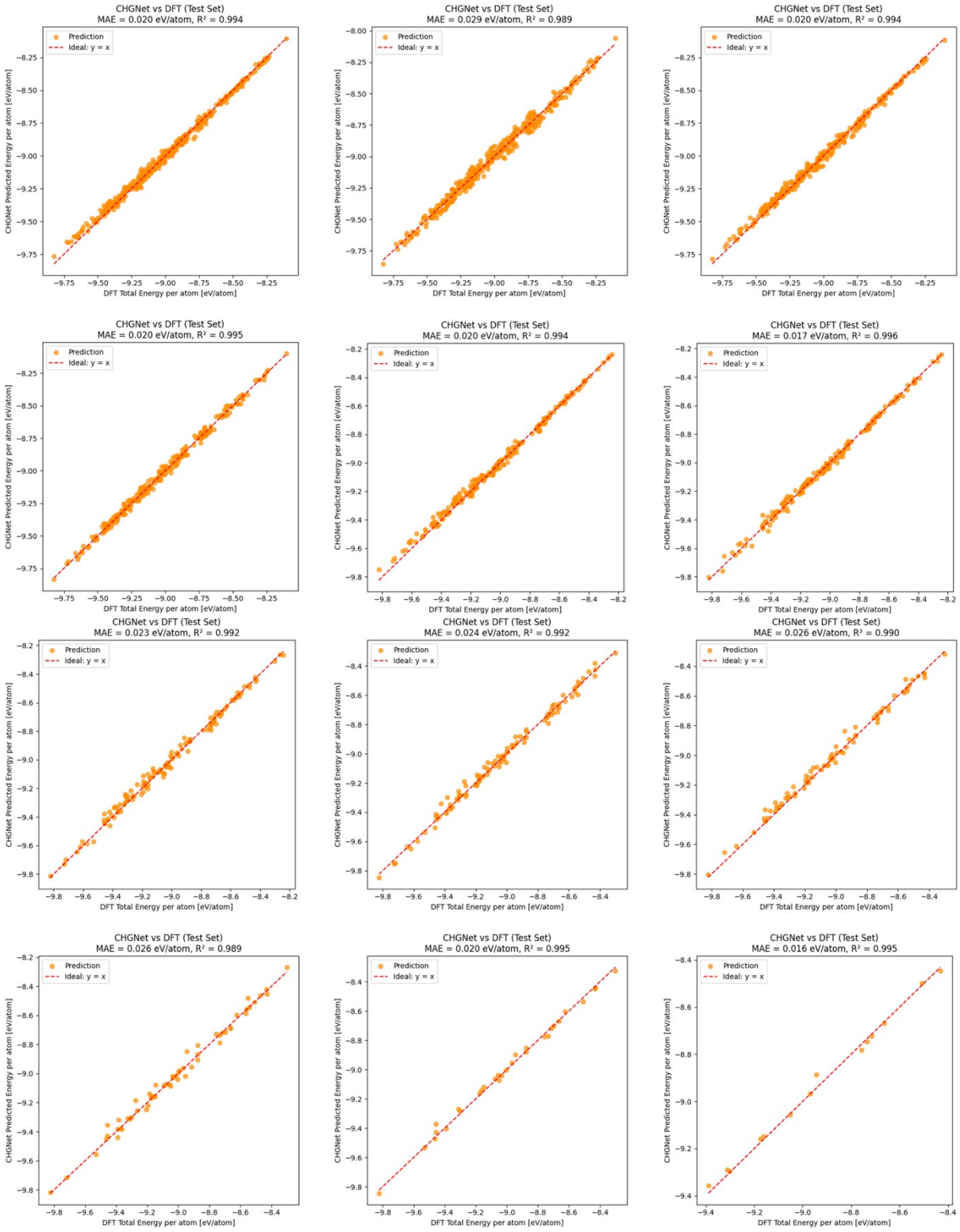

Figure S7. MAE and R^2 values after each iteration from 1 to 12 for Method 4.